Jour. Korean Earth Science Society, Vol. 23, No. 1, p. 87–96, January 2002

Subsurface Structure of the Yeongdong Basin by Analyzing Aeromagnetic and Gravity Data

Kyung-Jin Kim* and Byung-Doo Kwon

Department of Earth Science Education, Seoul National University, Seoul 151-742, Korea

Abstract: Aeromagnetic and gravity data were analyzed to delineate the subsurface structure of the Yeongdong basin and its related fault movement in the Okcheon fold belt. The aeromagnetic data of the total intensity (KIGAM, 1983) were reduced to the pole and three dimensional inverse modeling, which considers topography of the survey area in the modeling process, were carried out. The apparent susceptibility map obtained by three dimensional magnetic inversion, as well as the observed aeromagnetic anomaly itself, show clearly the gross structural trend of the Yeongdong basin in the direction on between N30°E and N45°E. Gravity survey was carried out along the profile, of which the length is about 18.2 km across the basin. Maximum relative Bouguer anomaly is about 7 mgals. Both forward and inverse modeling were also carried out for gravity analysis. The magnetic and gravity results show that the Yeongdong basin is developed by the force which had created the NE-SW trending the magnetic anomalies. The susceptibility contrast around Yeongdong fault is apparent, and the southeastern boundary of the basin is clearly defined. The basement depth of the basin appears to be about 1.1 km beneath the sea level, and the width of the basin is estimated to be 7 km based on the simultaneous analysis of gravity and magnetic profiles. There exists an unconformity between the sedimentary rocks and the gneiss at the southeastern boundary, which is the Yeongdong fault, and granodiorite is intruded at the northwestern boundary of the basin. Our results of gravity and magnetic data analysis support that the Yeongdong basin is a pull-apart basin formed by the left-stepping sinistral strike-slip fault, which formed the Okcheon fold belt.

Key words: Okcheon fold belt, strike-slip fault, unconformity, pull-apart basin

INTRODUCTION

The Yeongdong basin is distributed through Yeongdong-Gun at Chungchong-Pukdo, Sangju-Gun at Kyongsang-Pukdo, Muju-Gun at Jeunla-Pukdo (Fig. 1). This area is located on the border of southeastern part of Okcheon fold belt.

A few studies have been published on the characteristics of sediments and the depositional environments of the Yeongdong basin (Kim, 1973, 1974; Lee and Paik, 1989, 1990; Kim and Hwang, 1986; Kim and Lee, 1986). The Yeongdong basin is regarded to be formed in Late Jurassic to Early Cretaceous and to be a pull-apart basin accumulated in the collapsed area by a left stepping en-echelon sinistral fault. Judging from a series of major sinistral wrench faults developed in the southern part of Korean Peninsula, which are the probable exten-

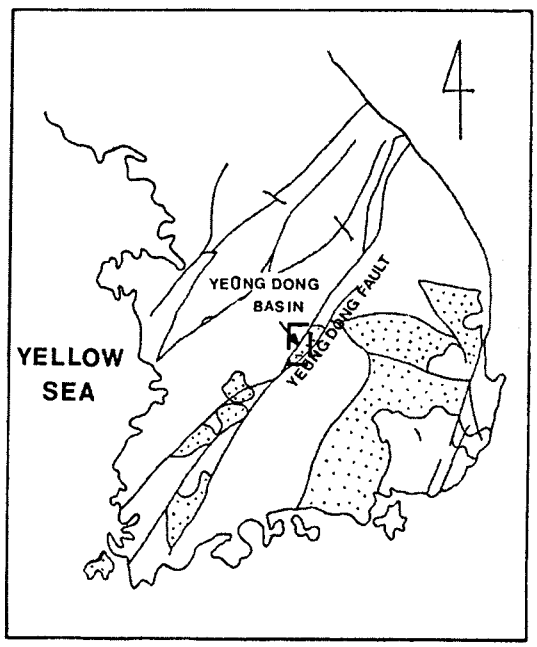

Fig. 1. Location map of the Yeongdong basin. Dotted areas are basins distributed in the southern part of Korean peninsula. Dashed line frame indicates the study area.

*E-mail: khammer_kr@yahoo.co.kr

sion of the Tancheng-Lujiang fault system characterizing by NE-SW structural trend in the continental margin of mainland China, these faults are inferred to be affected by its movement (Lee and Paik, 1989, 1990). Mann *et al.* (1983) have studied the basins developed by strike-slip faults and classified the basin types according to fault movements. Lee and Paik (1990) inferred the depth of the Yeongdong basin to be 6km according to sedimentological and statistical studies (Aydin and Nur, 1982, 1985). But geophysical studies have not been conducted to confirm this depth.

We have analyzed the aeromagnetic data of the basin and its adjacent area and carried out a gravity profiling to delineate the subsurface structure of the Yeongdong basin and its related fault movement in Okcheon fold belt. Aeromagnetic data were obtained by KIGAM in 1983. RTP (Reduction to the pole) and 3-D inverse modeling were performed to analyze aeromagnetic data. Simultaneous forward modeling using the Bouguer anomaly and magnetic anomaly were performed.

GENERAL GEOLOGY

Non-marine basins distributed throughout the southern part of the Korean Peninsula are commonly in contact with bedrocks bordering on their major faults. The strikes of these faults are mostly northeastern and the conditions of their extensions are very good. From this, it is deducted that these basins were developed by tectonic movements having same ages and same tensions (Lee and paik, 1989, 1990).

The study area (Fig. 1) is located on the border of southeastern of Okcheon fold belt. Figure 2 shows the geology of the Yeongdong basin and the neighboring area. The Yeongdong formations are in contact with Precambrian biotite gneiss (Pcbgn), granite gneiss (Pcggn), mica schist (sch) of Sobaiksan metamorphic complex on the border of the NE-SW trending Yeongdong fault. Mica granite (mgr) and porphyritic granite (pgr) widely distributed in the north-

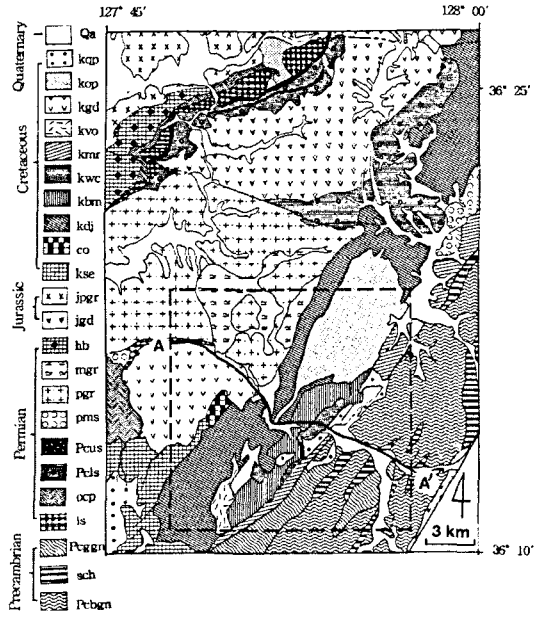

Fig. 2. Geology of the Yeongdong basin and its neighboring area. Line A-A' indicates the gravity survey profile. Dashed line frame indicates the section for magnetic inversion.

western side of the Yeongdong basin are age-unknown, but these are composed of the bedrock of the Yeongdong formations. So, it can be deduced that these were formed before the Cretaceous. Hornblendite (hb) are controversial area for its origin and age.

The Yeongdong formations are composed of Myungyundong Formation (kmr), Wonchonri Formation (kwc), Paekmasan Formation (kbm), Dongjungri Formation (kdj) and Saniri Formation (kse, co). Most of these formations are composed of shale, sandstone and conglomerate. But exceptionally Wonchonri Formation is composed of tuff-sandstone. Orthophyre (kop) is largely developed in the NE-SW subparallel aspect within the basin. These factors will affect the interpretation of magnetic and gravity data.

MAGNETIC ANALYSIS

Qualitative Analysis of Aeromagnetic Data

Figure 3 shows the residual magnetic anomaly map obtained after removing the IGRF (Interna-

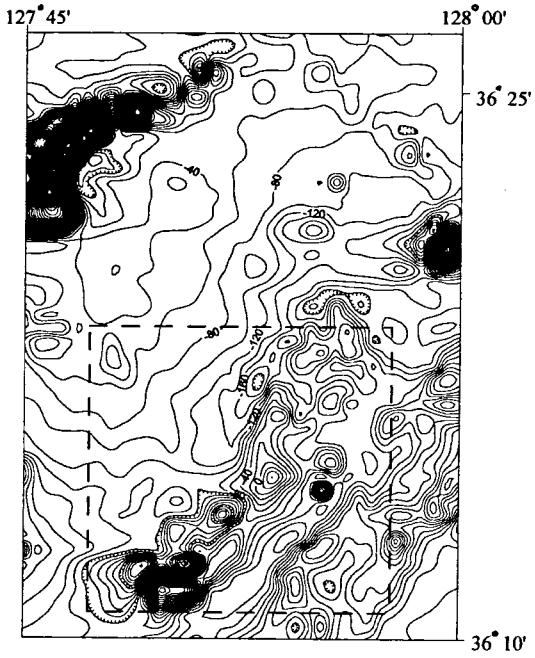

Fig. 3. Aeromagnetic anomaly of the Yeongdong basin and its neighboring area of Fig. 2. Contour interval is 20 nT. Dashed line frame indicates the section for magnetic inversion.

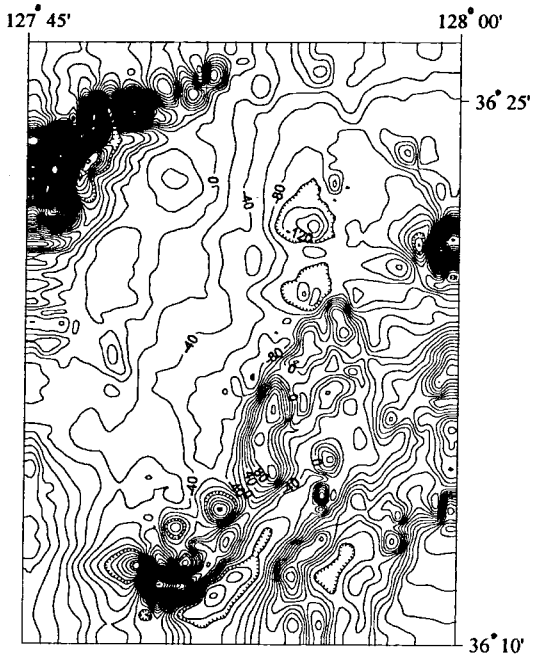

Fig. 4. RTP (Reduction to the pole) processed magnetic anomaly in Fig. 3. Contor interval is 20 nT.

tional Geomagnetic Reference Field, 1980) from observed aeromagnetic data. Flight was carried out at the altitude 400 feet above the topography with 1km interval and magnetic measurements were made with grid spacing of 500 m by using a Geometrics G-813 proton magnetometer.

Aeromagnetic anomaly map shows several characteristics. High magnetic anomalies appear in the northwestern corner where hornblendite are exposed. Because hornblendite commonly has very high susceptibity, it shows high magnetic anomaly regardless of topography. The Yeongdong basin shows low anomalies, because of low susceptibities of sedimentary rocks. The gross trend of magnetic anomalies are developed in the NE-SW direction, and this pattern is well coincide with geology and topography. Western Wonchonri formation, however, shows relatively high magnetic anomaly comparing with other formations in the basin, and it is thought to be of volcanic origin.

Since the aeromagnetic surveys measure the total intensity of the magnetic field, we transformed the observed anomalies into the RTP (reduction to the pole) anomalies. The RTP process converts magnetic data recorded in the inclined earth's magnetic field to what the data would have looked like if the magnetic field had been vertical (Gunn, 1975). Therefore, reduced-to-pole data have advantage over the original data in delineating the linear characteristics of geologies such as fault boundaries. Figure 4 is RTP transformed anomaly of Fig. 3, which shows the magnetic anomalies, on the whole, are slightly shifted to the northwest. Comparing with the geology, we can recognize that the boundaries of the Yeongdong are more clearly identified on the RTP map.

Inversion of Magnetic Data

Magnetic effect is sensitive to the topography where surface rocks are non-sedimentary and then magnetic anomalies can seriously be deformed (Grauch and Campbell, 1984; Park, 1992). Altitudes of the

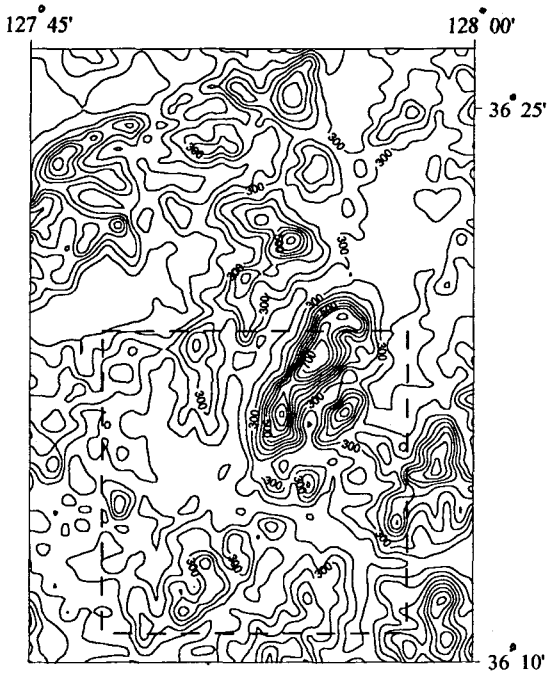

Fig. 5. Topography of the Yeongdong basin and its neighboring area. Contour interval is 50 m. Dashed line frame indicates the section for magnetic inversion.

study area are between 100 m and 980 m and irregularities of topography are relatively serious (Fig. 5). Therefore, it needs to consider the magnetic effects of the topography in analyzing the magnetic anomalies quantitatively.

Various methods have been developed to analyze aeromagnetic anomaly data, but only a few programs involving topographic corrections of the complex geology have been proposed. Plouff (1976) calculated magnetic effects using least-square methods in area where susceptibilities are unknown, but this method is only valid if the thickness of the prism is less than the height of the computation points above them. The method by Parker (1972) depends on the topography and its magnetic effect being related by a Fourier transform, but it is only appropriate if the calculation points are above the highest point in the topography. Grauch (1987) also developed a program for removing the effects of topography where the target sources have no relation to the topography. But, if susceptibility distributions vary with the terrain which is related to the geology of the survey area, interpretation errors are occurred.

In this case, it needs to analyze the magnetic anomaly with considering topography. Because the target sources in this study is the sedimentary basin which is outcropped on the rugged surface, we have modified Woodward's method (Woodward, 1993) to develop a susceptibility inversion program considering the topography effects during the inversion process. The topographic model used by Woodward is comprised of vertical line elements which are different in height and magnetization varying with the position. But his aeromagnetic data of White Island in New Zealand were obtained with the grid spacing less than 100 m, flight height less than 60 m above terrain and flight interval less than 100 m, of which samples are much denser than ours. Therefore, we introduced a vertical prism model instead of the vertical line element. Each vertical prism can be varied with terrain height, susceptibility, and depth and three dimensional susceptibility inversion has been carried out using the Marquart-Levenberg method (Lines and Treitel, 1984).

The magnetic effect of the topography at a grid point (p, q) is defined as F

$$F_{pq} = \sum_{s=-k}^{k} \sum_{t=-k}^{k} U_{s,t} m_{p-s,q-t} \quad (1)$$

Where U is green function indicating the magnetic effect of a single grid of unit susceptibility and k is sufficiently large that contributions from more distant grid points can be neglect. By using the matrix form, the equation (1) can be shown

$$F = Km \quad (2)$$

Where F is a one-dimensional (1-D) array containing the known anomalies at grid points within n ($n \geq k$) of a specific grid point (i, j) and m is the susceptibility at the grid points within ($k + n$) of (i, j). K is a 2-D array with the appropriate elements of the green's function U. The dimensions of F and m are ($2n + 1$) and ($2k + 2n + 1$), respectively. The values of F (observed magnetic anomaly) are known.

So equation (2) can be treated as an underdetermined set of equations for the susceptibility in the vicinity of (i,j).

To obtain an approximate solution for the susceptibility valid for the field point (i, j), the equations must be constrained. This is achieved by equating the susceptibility of all elements more than n sample points from the field point to those on the boundary of this area. As these elements are distant from the field point, their effects are negligible in computing the susceptibility at the field point. This constraint is sufficient to make the rank and number of unknowns in the equations equal.

Equation (2), as modified by the constraints, is then inverted so that

$$m = \overline{K}^{-1}F \qquad (3)$$

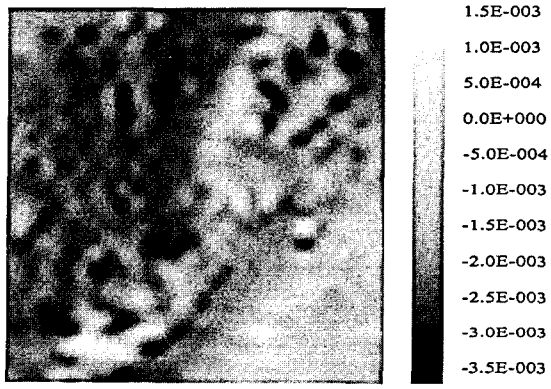

Fig. 6. Gray map of the apparent susceptibilities calculated by three dimensional inversion of magnetic data in the section indicated by dashed line frame in Fig. 3.

Where $\overline{K}$ is modified form of K by the application of the constraints and $\overline{K}^{-1}$ is the pseudo-inverse

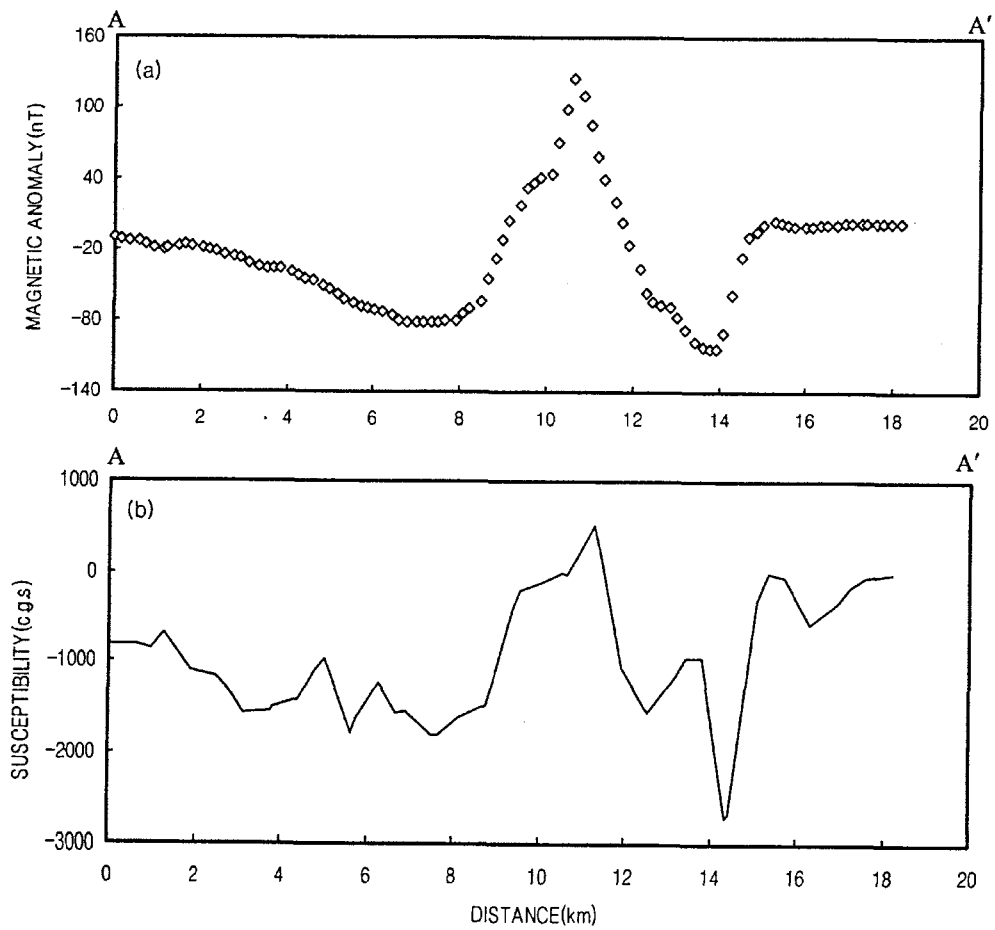

Fig. 7. (a) Aeromagnetic anomaly and (b) Apparent susceptibility of A-A' profile in Fig. 2.

of $\overline{K}$. The absolute value of magnetization is influenced by depth, but we do not know the depths of model prisms. Therefore, the result obtained from the inversion is not the real susceptibility but apparent susceptibility. But the aspect of apparent susceptibility is similar with that of real susceptibility in interpreting the geology. In this study, the depth of each model prism is assumed to be 2 km constant below the sea level.

For inversion we selected a portion of regular square of 15 km × 15 km in the aeromagnetic map, which includes the gravity profile (see Figs. 2, 3 and 5). The total number of sample data is 30 × 30.

Figure 6 shows the distribution of apparent susceptibilities. Comparing with Figs. 2 and 3, the apparent susceptibilities of the Yeongdong basin are different from the general appearance of other sedimentary basins. This is mainly due to the effects of andesite volcanic rock and orthophyre having high susceptibilities which cover large part of surveyed area. But, in general, the apparent susceptibility map shows the structural trend of NE-SW more clearly than the aeromagnetic anomaly map itself. Also the susceptibility contrast between the basin and the bedrock around the Yeongdong fault is apparent and the southeastern boundary of the Yeongdong basin is clearly defined.

Figure 7 shows the apparent susceptibility samples along the gravity profile A-A' indicated in Fig. 2. But this magnetic susceptibility profile does not show any typical characteristics of the basin; instead, it shows the high susceptibility reflecting the high magnetic anomaly around the basin. Considering the geology (Fig. 2), this high anomaly is thought to be due to the intruded volcanic rocks.

GRAVITY ANALYSIS

Inversion of Gravity Data

Gravity survey was conducted by using a Lacoste-Romberg gravimeter, of which accuracy is 0.01 mgal. The gravity profile is about 18.2 km throughout latitude 36°12' ~ 36°17' and longitude 127°47' ~ 127°58' crossing the Yeongdong basin (Fig. 2). Rock samples were collected at the 22 gravity stations to measure the densities of the rocks (Table 1).

Table 1. Densities of rocks distributed in the survey area

Rock type	Mean density (g/cm^3)	Density range (g/cm^3)
Tuff-sandstone	2.55	2.54 ~ 2.56
Precambrian granite gneiss	2.62	2.50 ~ 2.67
Granodiorite	2.74	2.72 ~ 2.75
Sandstone, conglomerate	2.70	2.69 ~ 2.72
Limetone	2.80	2.69 ~ 2.90

The densities of Wonchonri Formation composed of tuff-sandstone are very low, but those of the other Yeongdong formations composed of sandstone and conglomerate are some high. The field gravity measurements were reduced to Bouguer anomaly by application of drift, tidal, free-air, Bouguer and terrain corrections (Fig. 8a). The relative maximum Bouguer anomaly appeared on this profile is about 7mgals. The low anomalies on the central part reflect the Yeongdong basin, and especially around the Wonchonri Formation and the fault comprising the southeastern boundary, the changes of anomaly contrast are apparent. This will be thought of the low densities of Wonchonri Formation and fracture zone. The northwestern boundary of the basin is not apparent than the southeastern boundary because of low density-contrast between the granodiorite and the Yeongdong formations of sandstone and conglomerate.

Inverse and forward modeling were carried out for gravity analysis (Fig. 8). Measured densities of the rock samples were used to obtain the outline of the basin by forward modeling. And average depth of basin is assumed to be about 1.1 km from the result of rough forward modeling. Inversion of gravity data is to define the underground sources from the observed data using the model parameters such as densities or depth. In this study, the least-square inversion, based on Marquardt-Levenberg method (Lines and Treitel, 1984), was carried out by using 37 × 4 rectangular prism models.

Figure 8(b) shows the result of subsurface den-

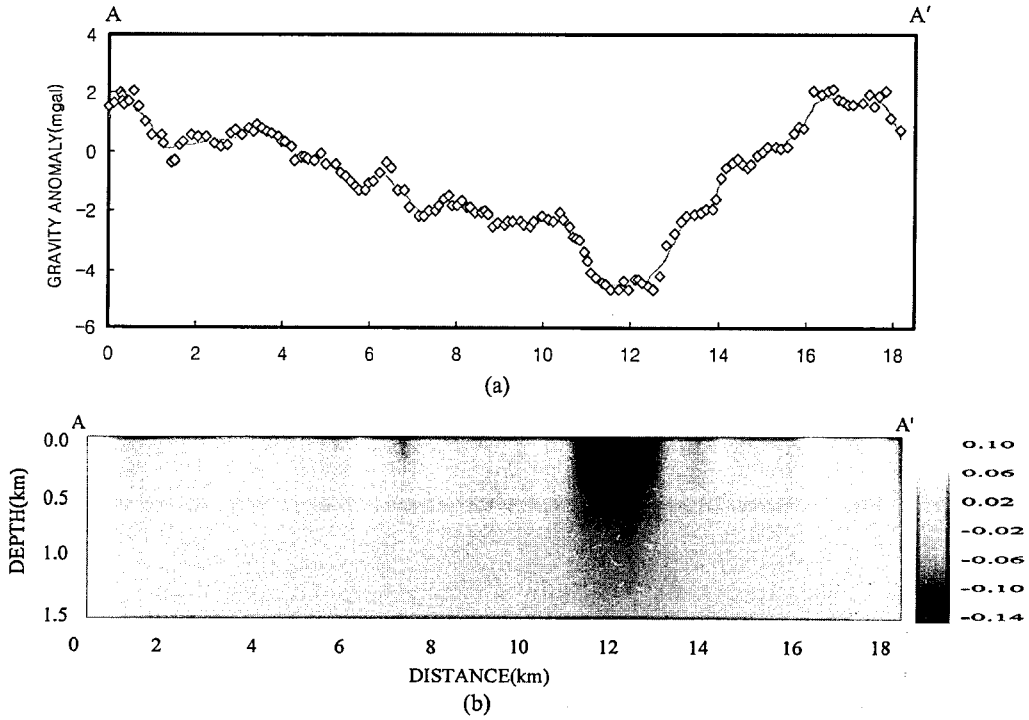

Fig. 8. Bouguer anomalies (a) and subsurface density section (b) of the profile A-A'. Diamond symbols indicate the observed gravity anomalies and the solid line indicates the calculated anomalies from the subsurface density structure obtained gravity inversion. Gray scale of density contrast is g/cm^3.

sity contrast obtained by gravity inversion. The calculated values are not exactly matched to observed data because of the limit of the shape and the size of prism. But the outline of density distributions looks reasonable. Density contrasts range from –0.15 g/cm^3 to 0.10 g/cm^3, and the highest density contrast is seen at around the distance of 12 km. As mentioned above, it can be said that the southeastern boundary of the Yeongdong basin does show the large density contrast between low density sedimentary rocks and adjacent metamorphic rocks. But, the northwestern boundary of the basin is not so distinct because of the intrusion of granodiorite in late Cretaceous and low density contrasts between sedimentary rocks of conglomerate and sandstone and granites. Comparing with the results of magnetic inversion (Fig. 7), the density contrasts implying volcanic rocks, which have large magnetic susceptibility, do not appear.

THE GEOPHYSICAL MODEL OF THE YEONGDONG BASIN

The detailed subsurface structure of the Yeongdong basin was modeled by simultaneous two-dimensional forward modeling using both gravity and magnetic data (Fig. 9). The optimum result is obtained by repetitive adjustments of outlines of rock masses, density and susceptibility contrasts of each rock type. The geologic map of Fig. 2 is used as constraints of outcrops of rock formations on this profile.

Andesite volcanic rock around the western Wonchonri Formation shows high susceptibility, but Dongjungri Formation shows also relatively high susceptibility unexpectedly. High Bouguer anomalies on left and right ends of the profile are resulted from high density of limestone and gneissic rock, respectively. Low gravity anomalies in the center of the

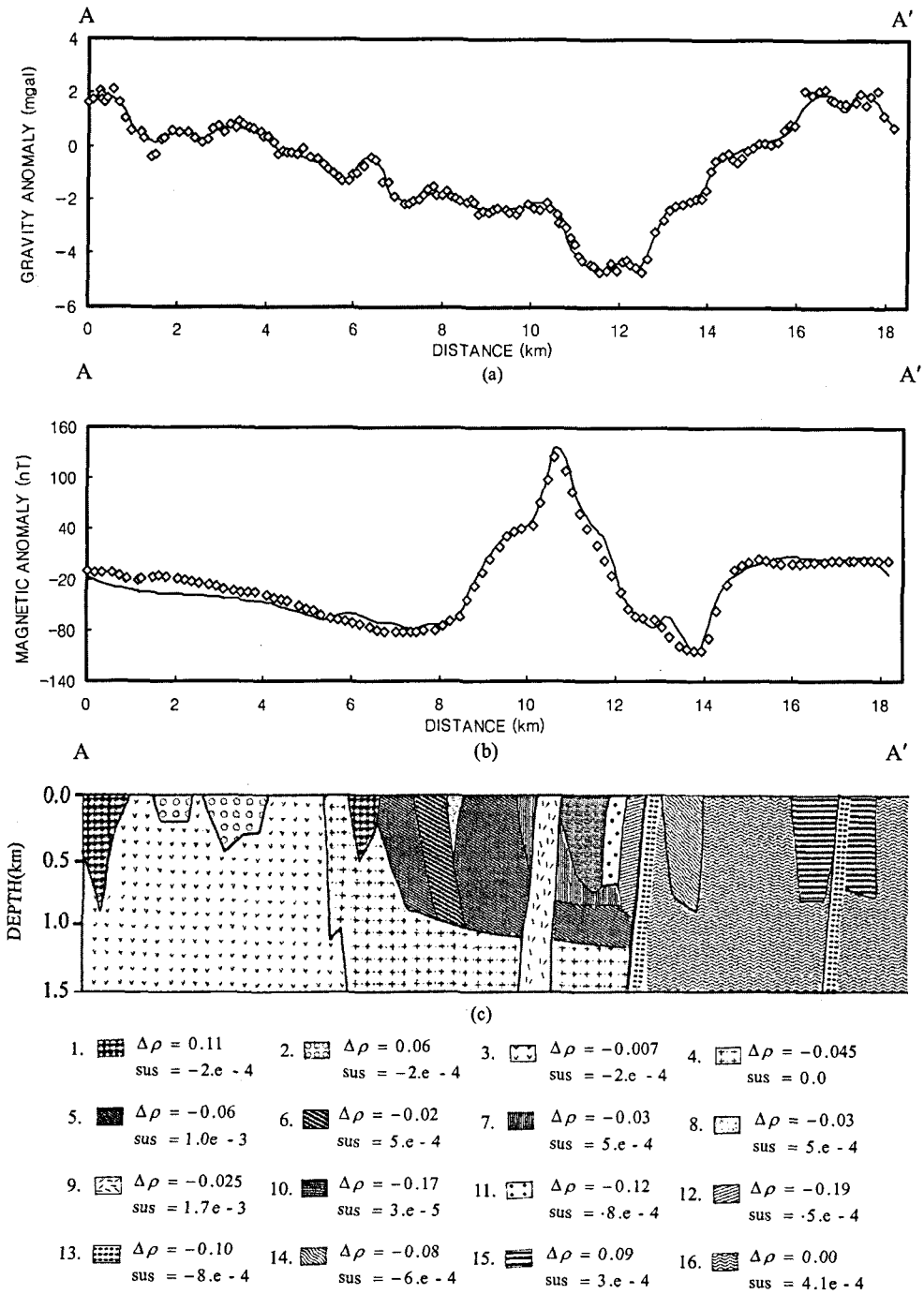

Fig. 9. (a) Bouguer gravity anomalies. (b) Magnetic anomalies. Diamond symbols and solid lines indicate observed anomalies and calculated anomalies, respectively. (c) Optimum geophysical (density and susceptibilities) model of subsurface structure of the Yeongdong basin obtained by repetitive forward calculation. Δρ is density contrast (g/cm^3) and sus is susceptibility (c.g.s). 13th index indicates fracture zone and the other indexes of lithology are same as those in Fig. 2.

profile are due to tuff-sandstone in Wonchonri Formation (kwc) and conglomerate, sandstone, and shale in Dongjungri (kdj) and Paekmasan formations (kbm), which are accumulated in the Yeongdong basin.

The mass of granodiorite is appeared to intrude the porphyritic granite (pgr), bedrock of the basin. Also, comparing with geology, the boundary between sedimentary formations and gneiss of Sobaiksan metamorphic complex on the inversion result can be clearly inferred as a fault boundary. On the whole, the results of gravity and magnetic data analysis support the geologic model proposed by Lee and Paik (1989, 1990) that the Yeongdong basin has been developed through an en-echelon fault by the strike-slip fault and deposits has been accumulated in the collapsed area. Therefore, there is unconformity between Yeongdong basin and gniess, bedrock of this area.

CONCLUSION

Gravity and aeromagnetic data were analyzed to delineate the subsurface structure of the Yeongdong basin and its related fault movement in Okcheon fold belt. The three dimensional magnetic inversion was conducted by using the method which considers magnetic effects of terrains. Gravity survey was carried out along the profile of about 18.2 km across the Yeongdong basin.

The boundaries of the Yeongdong basin and NE-SW trend appear relatively well not only in geology but also on the aeromagnetic anomaly map, which can support that the Yeongdong basin is pull-apart basin developed by strike-slip fault. Apparent susceptibility map obtained by three dimensional magnetic inversion clearly show the gross structural trend of the basin. Also the susceptibility contrast between the basin and the bedrock around the Yeongdong fault is apparent and the southeastern boundary of the Yeongdong basin is clearly defined.

Maximum difference of relative Bouguer anomaly between sedimentary rocks accumulated in the basin and biotite gneiss of bedrock in the study area is about 5mgals. The depth to the basement appears to be about 1.1 km beneath the sea level and the width of the basin appears to be 7 km by simultaneous analysis of gravity and magnetic data. There exists an unconformity between the basin and gneiss at the southeastern boundary, which is the Yeongdong fault, of the basin.

The results of geophysical modeling of the Yeongdong basin using aeromagnetic and gravity profile data supports the geologists' idea that the Yeongdong basin is a pull-apart basin formed by the left-stepping sinistral strike-slip fault, which formed Okcheon fold belt. Our geophysical model infers the depth of basement is about 1.1 km beneath the sea level and clearly shows that, at the southeastern boundary of basin, the Yeongdong basin is bordered by the Yeongdong fault, and granodiorite body is intruded at the northwestern boundary of the basin.

ACKNOWLEDGMENTS

The authors wish to express gratitude to graduate members of geophysical research group of the Department of Earth Science Education of Seoul National University for their kind supports during field surveys.

REFERENCE

Aydin, A. and Nur, A., 1982, Evolution of pull-apart basins and their scale independence. Tectonics, 1, 1, 91–105.

Aydin, A. and Nur, A., 1985, The types and role of stepovers in strike-slip tectonics, Biddle, K.T. and Christie-Blick, N. (Eds.), strike-slip deformation, basin formation, and sedimentation. Society of Economic Paleontologists and Mineralogists, Special Publication, 37, 35–44.

Grauch, V.J.S. and Campbell, D.L., 1984, Does draping aeromagnetic data reduce terrain-induced effects?. Geophysics, 49, 75–80.

Grauch, V.J.S., 1987, A new variable-magnetization terrain correction method for aeromagnetic data. Geophysics, 52, 94–107.

Gunn, P.J., 1975, Linear transformations of gravity and magnetic fields. Geophysical Prospecting, 23, 300–312.

Kim, D.H. and Lee B.J., 1986, Geological report of the Chungsan Sheet (1:50000), Korea Institute of Energy and Resources.

Kim, H.M., 1973, Paleocurrent analysis of the Yeongdong Group, Southern Korea. Journal of the Geological Society of Korea, 10, 1–24.

Kim, H.M., 1974, Sedimentation of the Yeongdong Group,

Southern Korea. Journal of the Geological Society of Korea, 10, 225–244.

Kim, K.B. and Hwang, J.H., 1986, Geological report of the Yeongdong Sheet (1:50000), Korea Institute of Energy and Resources.

Lee, D.W. and Paik, K.H., 1989, Sedimentological characteristics along Yeongdong fault zone in Cretaceous Yeongdong basin, South Korea. Journal of the Geological Society of Korea, 25, 259–272.

Lee, D.W. and Paik, K.H., 1990, Evolution of strike-slip fault-controlled Cretaceous Yeongdong basin, South Korea. Journal of the Geological Society of Korea, 26, 257–276.

Lines, L.R. and Treitel, S., 1984, Tutorial: A review of least-squares inversion and its application to Geophysical problems. Geophysical Prospecting, 64, 2351–2355.

Mann, P., Hempton, M.R., Bradley, D.C., and Burke, K., 1983, Development of pull-apart basins. Journal of Geology, 91, 529–554.

Park, J.H., 1992, Terrain correction of magnetic data. Thesis of Korea National University, 76–78.

Parker, R.L., 1972, The rapid calculation of potential anomalies. Geophysical Journal of the Royal Astronomical Society, 31, 447–455.

Plouff, D., 1976, Gravity and magnetic fields of polygonal prism and application to magnetic terrain corrections. Geophysics, 41, 727–741.

Woodward, D.J., 1993, Inversion of aeromagnetic data using digital terrain models. Geophysics, 58, 645–652.

Manuscript received November 15, 2001
Revised manuscript received November 22, 2001
Manuscript accepted November 30, 2001